Compact-footprint, focusing, lithographically-scribed planar holographic Bragg reflector

C. Greiner*, D. Iazikov and T. W. Mossberg
LightSmyth Technologies, Inc., 860 W. Park St., Ste 250, Eugene, OR 97041

ABSTRACT

Planar holographic Bragg reflectors (HBR's) are slab-waveguide-based computer-generated two-dimensional in-plane refractive-index holograms. The slab waveguide allows signals to propagate freely in two dimensions, a geometry that enables HBR's to offer powerful holographic function in the form of simultaneous spectral and spatial signal processing in a single element. Owing to their planar structure HBR's are fully consistent with photolithographic fabrication which provides complete amplitude and phase control over individual diffractive elements thus providing a flexible means to precisely engineer device spectral transfer functions. Here, we report on a photolithographically-fabricated silica-on-silicon slab-waveguide-based HBR that provides 17 GHz, essentially Fourier-transform limited, spectral resolution in a device footprint of only 0.3 cm^2. The device maps the input beam to a spatially distinct output with diffraction-limited performance. Our results conclusively establish that the silica-on-silicon format and submicron photolithography can provide fully coherent planar holographic structures of centimeter scale.

Keywords: Integrated Optics, Bragg Reflector, Planar Waveguide, Lithography, Holography

1. INTRODUCTION

Volume holograms provide many highly desirable functions for integrated photonic devices, such as single-element spatial and spectral processing of optical signals, low-loss input/output coupling based on efficient holographic wave front mapping as well as the ability to flexibly engineer device spectral transfer functions via diffractive element spatial arrangements. Yet, despite these inherent virtues, volume holographic devices have not made widespread impact in device technology, partly because of the generally difficult and complex interferometric recording methods typically required in fabrication and stability issues of the photoactive recording material.

Recently, it has been proposed[1,2] and demonstrated[3] that slab-waveguide-based planar holograms in the form of 2D holographic Bragg reflectors (HBR's) offer the same spectral and spatial processing capabilities as their fully three-dimensional counterparts while offering breakthrough pathways to fabrication. The planar HBR's of interest here consist of computer-generated, two-dimensional, etched gratings that are located within a slab waveguide. In the slab waveguide, light can propagate without constraints in two dimensions – a geometry that allows 2D Bragg structures to provide powerful planar holographic functions. A single HBR can be used to simultaneously spatially map (image) an input beam onto an output port (or from point-to-point within an integrated optical circuit) while at the same time providing spectral filtering. HBR structures, whose computer-generated diffractive contours provide broad in-plane spatial wavefront transformation capability, contrast with previously discussed 2D distributed Bragg reflectors intended for out-of-plane applications such as laser feedback and outcoupling[4-6] and free-space to slab-waveguide beam coupling[7,8]. The holographic imaging function made possible by HBR's is generally more powerful than that provided by confocal elliptical DBRs previously discussed in the context of spectral multiplexing[9].

Owing to their planar, typically surface relief, structure, HBR's are consistent with fabrication by photolithography and low-cost mass production via nanoreplication techniques such as hot embossing[10-12]

* e-mail: cgreiner@lightsmyth.com; phone: (541)-431-0026; fax: (541)-284-5607

or nanoimprint lithography[13]. In contrast to UV-written grating structures (e.g. fiber Bragg gratings)[14-17], photolithography allows gratings to be written with complete amplitude and phase control over individual diffractive elements. Lithographically scribed HBR's can therefore provide a means of producing low-cost devices with very complex spectral transfer functions, e.g. tailored bandpass shapes. Unlike fiber and channel-waveguide gratings[18-19], where separation of the counter-propagating input and output signals typically requires a bulky circulator or a lossy power splitter, planar HBR devices have distinct and separately accessible input and output ports allowing convenient low-loss separation of the signal from the input on the same substrate. HBR spectral resolution scales inversely with device length and waveguide refractive index. Spectral resolution of ~10 GHz is expected from fully-integrated silica-on-silicon devices of only a centimeter in length.

We report here on a lithographically-fabricated slab-waveguide holographic Bragg reflector that provides 17 GHz, essentially Fourier-transform-limited, spectral resolution in a device footprint of only 0.3 cm^2 and focuses the resonant input beam to a spatially distinct output with diffraction-limited performance.

2. RESULTS AND DISCUSSION

In Figure 1a we show a schematic HBR cross section. It consists of a silica slab waveguide with a central core of thickness w ≈ 6 μm and bilateral 15-μm-thick cladding layers. The core (cladding) index, n_{core} (n_{clad}), of ~1.46 (~1.446) for the wavelength of 1.55 μm yields a core-cladding index differential, Δ, of ~0.8 %. Figure 1a also depicts cross-sections of representative lithographically-scribed diffractive contours located at the upper core-cladding interface. The diffractive contours, with depth, d ≈ 450 nm, consist of trenches filled with cladding material. The device operates in first order with a contour spacing, Λ, of about

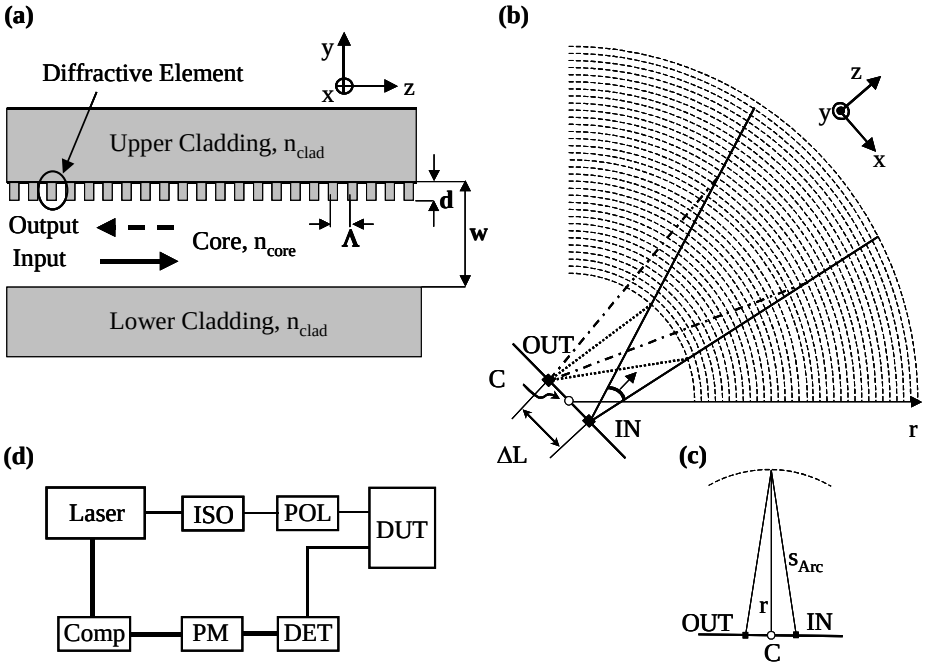

Figure 1. Planar Holographic Bragg Reflector Schematic. 1a, Cross-sectional view. 1b, Top view. IN (OUT), input (output) port; ΔL, input/output port separation; C, center of curvature of diffractive contours; 1c, Schematic illustrating relation between device optic axis, r, and optical path, s_{Arc}, to a given diffractive arc. 1d, Test setup; ISO, optical isolator; POL, polarization controller; DUT, device under test; DET, detector; PM power meter; Comp, Computer.

500 nm, i.e. one half of the in-medium wavelength of resonant light. Figure 1b is a top view of the planar HBR. An optical signal is coupled into the planar grating device via an input port, IN, which may lie either

in the interior or at the edge of the device die. In the former (latter) case, a channel waveguide (butt-coupled fiber) is used to inject signal into the slab region. The input beam expands in the slab region and is subsequently spectrally filtered and spatially directed to the output port, OUT, by the HBR. The HBR diffractive contours are represented by the dashed lines in Figure 1b, and can be designed individually to match the back-diffracted input field to the output port. The detailed spacing and relative amplitude of the diffractive contours as a function of position along the input direction determine the spectral transfer function of the device. Specifically, in the limit of weak device reflectivity, the HBR spectral transfer function is proportional to the spatial Fourier transform of the diffraction contour amplitude distribution[1]. In the tested device, the contours are circular arcs which are concentric about center of curvature, point C. Adjacent HBR diffractive contours are spaced such that the optical path length s_{Arc} (see Figure 1c) is incremented by a constant amount Λ from one arc to the next. Consequently, the spacing between adjacent arcs, as measured along the device optic axis r, is weakly chirped. The HBR will in principle provide imaging between any input-output port pair symmetrically located about point C, but the weak chirp introduced during design to equalize contour-to-contour optical path increments will function optimally only at the design port separation, ΔL = 400 um. Unless otherwise noted all results shown were taken for this port separation.

Figure 1d is a test setup schematic. Light from a tunable laser (HP 8168F) is passed through an isolator and a polarization controller (Agilent 11896A) and injected into the HBR. The HBR output is detected by an Agilent 81625A optical head connected to an Agilent 8163A power meter. For spectral-transfer-function measurements the laser wavelength is stepped in 5 pm increments across the HBR resonance width. The purity of the linearly polarized input, P_p/P_o, where P_p (P_o) is the power along (orthogonal to) the test direction, was ~ 650.

In Figure 2 we explore the focusing properties of a 7-mm-long planar HBR with ~13300 grating lines that was fabricated by standard photolithography using a DUV optical stepper. The device occupies a footprint of about 9×3 mm^2 (length by width). For these measurements, the device die was cut so that (within a dicing tolerance of about 30 um) the die edge contains the center of curvature of the diffractive contours and lies normal to the optic axis. No channel waveguides are present. A butt-coupled SMF-28 fiber, approximately positioned 200 um to one side of the center of curvature, is used to inject signal. A second butt-coupled SMF-28 fiber, with tip at the immediate die edge, is scanned parallel to same edge around the nominal output focusing position, located 200 um to the opposite side of point C. Squares and error bars shown in Figure 2 represent mean power and standard deviation of five measurements of the HBR spatial output profile. Also shown as a dashed line is the measured output profile of the SMF-28 fiber used as input to the device. Figure 2 shows that the holographic Bragg reflector produces a focused output power profile closely approximating the input power distribution .

To compare test results with expected device performance we present in Figure 2b the modeled - based on Huygens-Fresnel diffraction theory - device spatial output behavior. A field with Gaussian transverse distribution (1/e- field diameter 10.4 μm), approximating the input fiber field distribution of the measurement, was used as input. Figure 2b, solid (dashed) line, shows the calculated HBR output (input) power profile convolved with the model fiber power profile. The dotted line in Fig 2b represents the directly calculated (unconvolved) spatial HBR output profile. As can be seen, the convolved output power profiles of model HBR and model input fiber exhibit very similar shapes and widths, consistent with the unity conjugate ratio expected on basis of simple imaging theory. The essentially identical measured and modeled focusing properties of Figure 2 demonstrate that the spatial input/output beam mapping provided by the fabricated holographic Bragg reflectors is limited only by basic diffraction theory.

In Figure 3, we present (solid line) the measured spectral transfer function of the 7-mm-long planar HBR. Channel waveguides ending at the locations of input and output port were used to launch and collect the signal. The graph depicts the device insertion loss as a function of wavelength for TE input polarization. The resonant insertion loss of the device was measured to be –3.1 dB, arising principally from low diffractive coupling strength that can be increased, for example, by lengthening the grating, reducing core thickness, increasing grating etch depth, increasing core-cladding index contrast, or placing the diffractive elements within the core. The fiber-to-channel-waveguide coupling loss was measured to be -1.4 dB and is subtracted from the results shown in Figure 3.

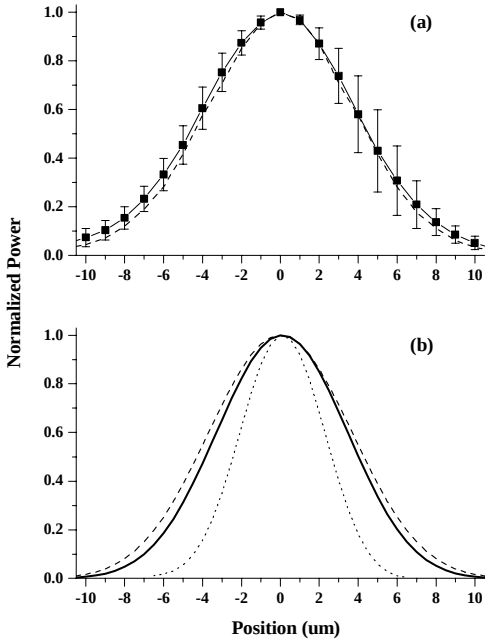

Figure 2. Measured and calculated HBR output spatial profiles. 2a, squares, HBR data; dashed line, measured input fiber spatial power profile. 2b, solid line, calculated HBR spatial output profile; dashed line, calculated input spatial power profile; dotted line, calculated unconvolved HBR output profile.

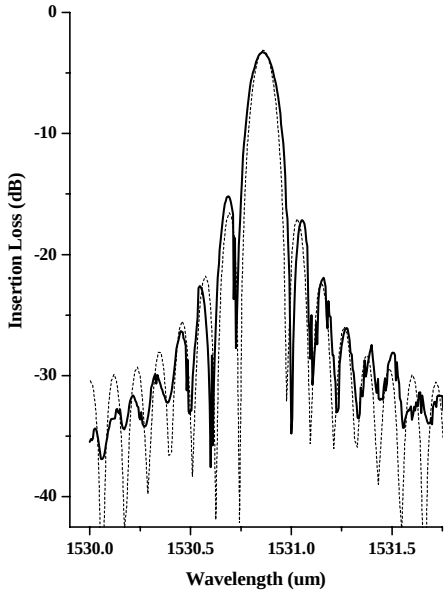

Figure 3. Solid line, measured insertion loss versus wavelength for a 7-mm long planar holographic Bragg reflector (TE polarization). Dashed line, spectral transfer function calculated by Huygens-Fresnel diffraction theory.

As seen in Figure 3, the 7-mm-long HBR has a spectral Full-Width-at-Half-Maximum of ~ 0.13 nm, corresponding to a fractional spectral resolution, $\Delta\lambda/\lambda$, better than 10^{-4}, close to the Fourier-transform-limited fractional bandpass of 7.5×10^{-5}, calculated for a one-dimensional grating with 13305 grating lines. The result of Figure 3 indicates that the lithographic fabrication process provides control at the same level of precision over imaging fidelity, feature placement, and index homogeneity over the device length. The

accuracy of the measured center wavelength of ~ 1.5308 μm as compared to the design value of 1.53037 μm is better than 3×10^{-4} and can be improved using the present results as calibration.

Figure 3, dashed line, is the modeled device spectral transfer function, calculated for the output port center using two-dimensional Huygens-Fresnel diffraction theory. An input field with Gaussian transverse distribution (1/e-diameter 12 μm) was assumed. All other simulation parameters match device parameters. The agreement between modeled and measured response is excellent. The measured transfer function is slightly broader than that of the model. This is likely the result of input field depletion not taken into account in the weak-reflection-limit-based model. The result of Figure 3 conclusively demonstrates that the silica-on-silicon format and submicron lithographic fabrication can provide fully coherent planar holographic structures of centimeter scale.

Figure 4 shows the HBR spectral transfer function for port separations other than the design separation. The solid (dashed) lines in Figure 4 (a) – (c) show test data (calculated behavior) for separations ΔL = 0 um (retro-reflection), 200 um and 600 um. Since the diffractive contour spacing is not optimized for these separations, but rather appears weakly chirped, the band passes are generally much broader than for ΔL = 400 um, the resonance centers are slightly shifted from the design value and they exhibit fairly high insertion loss.

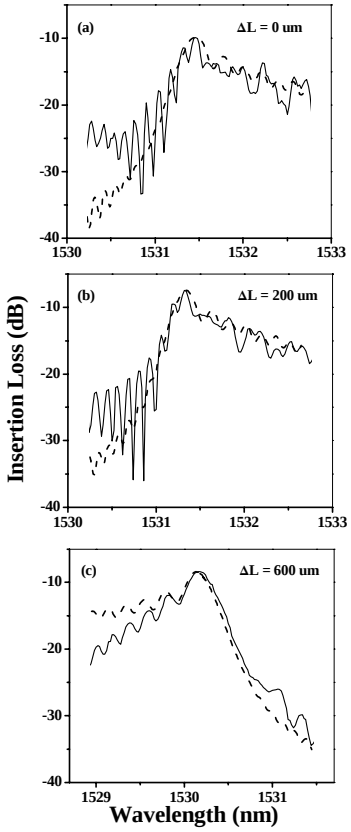

Figure 4. 4a – c, HBR spectral transfer function for port separations ΔL = 0 um (retro-reflection), 200 um and 600 um. Solid (dashed) lines, test data (modeled response).

III. CONCLUSIONS

In conclusion, we have demonstrated lithographically-fabricated silica-on-silicon-based holographic Bragg reflectors that provide spectral filtering performance and spatial beam mapping constrained only by the fundamental limits of Fourier transform and diffraction theory. We envision HBR's as constituting the basis of a fully 2D "photonic fabric" that provides not only many optics-on-a-chip functionalities such as WDM mux/demux, add-drop mux, temporal pattern recognition/generation via optical cross-correlation for packet switching, spectral LED slicing, on-chip laser wavelength locking, but also has the potential to integrate a variety of optical components into a single channel-waveguide-free format, thereby creating a pathway to highly-integrated ultra-compact photonic circuits.

REFERENCES

1. T. W. Mossberg, "Planar holographic optical processing devices", *Opt. Lett.*, vol. **26**, pp. 414 – 416, 2001.

2. T. W. Mossberg, "Lithographic Holography in Planar Waveguides", *SPIE Holography Newsletter*, vol. **12**, pp.1 and 8, 2001.

3. C. Greiner, D. Iazikov, and T. W. Mossberg, "Lithographically scribed, focusing, planar holographic Bragg reflector with 17-GHz passband and 0.3 cm2 footprint," presented at the Optical Fiber Communication Conference, post-deadline paper PD31, Atlanta, Georgia, USA, March 23-28, 2003.

4. T. Erdogan and D. G. Hall, "Circularly Symmetric Distributed Feedback Laser: Coupled Mode Treatment of TE Vector Fields," *J. Quant. Electron.*, vol. **28**, pp. 612-623,1992.

5. R. H. Jordan, D. G. Hall, O. King, G. Wicks, and S. Rishton, "Lasing behavior of circular grating surface emitting semiconductor lasers," *J. Opt. Soc. Am. B*, vol. **14**, pp. 449-453, 1997.

6. S. Kristjansson, N. Eriksson, A. Larsson, R. S. Penner, and M. Fallahi, "Observation of stable cylindrical modes in electrically pumped circular grating-coupled surface-emitting lasers," *Appl. Opt.*, vol. **39**, pp.1946-1953, 2000.

7. M. Li, B. S. Luo, C. P. Grover, Y. Feng, and H. C. Liu, "Waveguide grating coupler with a tailored spectral response based on a computer-generated waveguide hologram," *Opt. Lett.*, vol. **24**, pp. 655-657, 1999.

8. J. Backlund, J. Bengtsson, C. Carlstrom, and A. Larsson, "Input waveguide grating couplers designed for a desired wavelength and polarization response," *Appl. Opt.*, vol. **41**, pp. 2818-2825, 2002.

9. C. H. Henry, R. F. Kazarinov, Y. Shani, R. C. Kistler, V. Pol, and K. J. Orlowsky, "Four-channel wavelength division multiplexers and bandpass filters based on elliptical Bragg reflectors", *J. Lightwave Technol.*, vol. **8**, pp. 748 – 755, 1990.

10. J. Liu, Y.-L. Lam, Y.-C. Chan, Y. Zhou, B. S. Ooi, G. Tan, and J. Yao, "Embossed Bragg gratings on organically modified silane waveguides in InP", *Appl. Opt.*, vol. **39**, pp. 4942 - 4945, 2000.

11. R. Waldhäusl, B. Schnabel, P. Dannberg, E.-B. Kley, A. Bräuer, and W. Karthe, " Efficient coupling into polymer waveguides by gratings", *Appl. Opt.*, vol. **36**, pp. 9383 – 9390, 1997.

12. M.T. Gale, "Replication Technology for Holograms and Diffractive Optical Elements", *J. Imag. Sci. and Technol.*, vol. **41**, pp. 211 – 220, 1997.

13. J. Wang, S. Schablitsky, Z. Yu, W. Wu, and S. Y. Chou, "Fabrication of a new broadband waveguide polarizer with a double-layer 190 nm period metal-gratings using nanoimprint lithography", *J. Vac. Sci. Technol. B*, vol. **17**, 2957 – 2960, 1999.

14. T. Erdogan, "Fiber Grating Spectra, "*J. Lightwave Tech.*, vol. **15**, pp. 1277-1294, 1997.

15. T. Komukai, K. Tamura, and M. Nakazawa, "An Efficient 0.04-nm Apodized Fiber Bragg Grating and Its Application to Narrow-Band Spectral Filtering," *Photonics Tech. Lett.*, vol. **9**, pp. 934-936, 1997.

16. C. Marra, A. Nirmalathas, D. Novak, C. Lim, L. Reekie, J. A. Besley, C. Weeks, and N. Baker, "Wavelength-Interleaved OADMs Incorporating Optimized Multiple Phase-Shifted FBGs for Fiber-Radio Systems," *J. Lightwave Tech.*, vol. **21**, pp. 32-39, 2003.

17. A. Grunnet-Jepsen, A. E. Johnson, E. S. Maniloff, T. W. Mossberg, M. J. Munroe, and J. N. Sweetser, "Fibre Bragg grating based spectral encoder/decoder for lightwave CDMA," *Electron. Lett.* , vol. **35**, pp. 1096-1097, 1999.

18. D. Wiesmann, C. David, R. Germann, D. Erni, and G. L. Bona, "Apodized Surface-Corrugated Gratings With Varying Duty Cycles," *Phot. Tech. Lett.*, vol. **12**, pp. 639-641, 2000.

19. D. Wiesmann, R. Germann, G. L. Bona, C. David, D. Erni, and H. Jackel, "Add-drop filter based on apodized surface-corrugated gratings," *J. Opt. Soc. Am. B*, vol. **20**, pp. 417-423, 2003.